Monatshefte für Chemie 137, 1453–1462 (2006)
DOI 10.1007/s00706-006-0538-5

Monatshefte für Chemie
Chemical Monthly
Printed in Austria

α-Ketoacid Intermolecular Hydrogen Bonding. Supramolecular Ribbons and Stacking in α-Pyrroleglyoxylic Acids

Nicholas T. Salzameda and **David A. Lightner***

Department of Chemistry, University of Nevada, Reno, Nevada, USA

Received March 29, 2006; accepted April 7, 2006
Published online October 30, 2006

Summary. Rarely-seen carboxylic acid to ketone intermolecular hydrogen bonding is found in crystal structures of α-pyrroleglyoxylic acids. 3,4-Diethyl-1*H*-pyrrole-2-glyoxylic acid, prepared by saponification of the reaction product between 3,4-diethylpyrrole and ethyl oxalyl chloride formed crystals that showed the uncommon carboxyl to ketone intermolecular hydrogen bonding, with the hydrogen-bonded α-pyrroleglyoxylic acids stacked neatly in layers. This α-ketoacid hydrogen-bonding pattern was repeated in (*Z*)-2,3,7,8-tetraethyl-10*H*-dipyrrin-1-one-9-glyoxylic acid, which also engaged in dipyrrinone-to-dipyrrinone intermolecular hydrogen bonding to form supramolecular ribbons in the crystal.

Keywords. Pyrrole; Dipyrrinone; Synthesis; X-ray crystallography.

Introduction

There are relatively few crystal structure determinations of α-ketoacids, of pyruvic acid and its analogs. Except for two examples, they show carboxylic acid dimers that do not involve the ketone carbonyl. These two exceptions are phenylglyoxylic acid and mesitylglyoxylic acid [1] that form catemeric arrangements shown in Fig. 1A. In connection with our studies of dipyrrinone acids called [*n*]-semirubins [2], we prepared a 10-oxo-[2]-semirubin (**1**) and its monopyrrole analog (**2**) (Fig. 1B), which formed crystals suitable for X-ray analysis. While solution studies indicate that **1** and **2** are monomeric in $CHCl_3$, in their crystals a unique type of intermolecular hydrogen bonding was found: carboxylic acid to ketone carbonyl. The solution and crystal structure studies presented in the following are apparently the first for pyrrole glyoxylic acids.

* Corresponding author. E-mail: lightner@scs.unr.edu

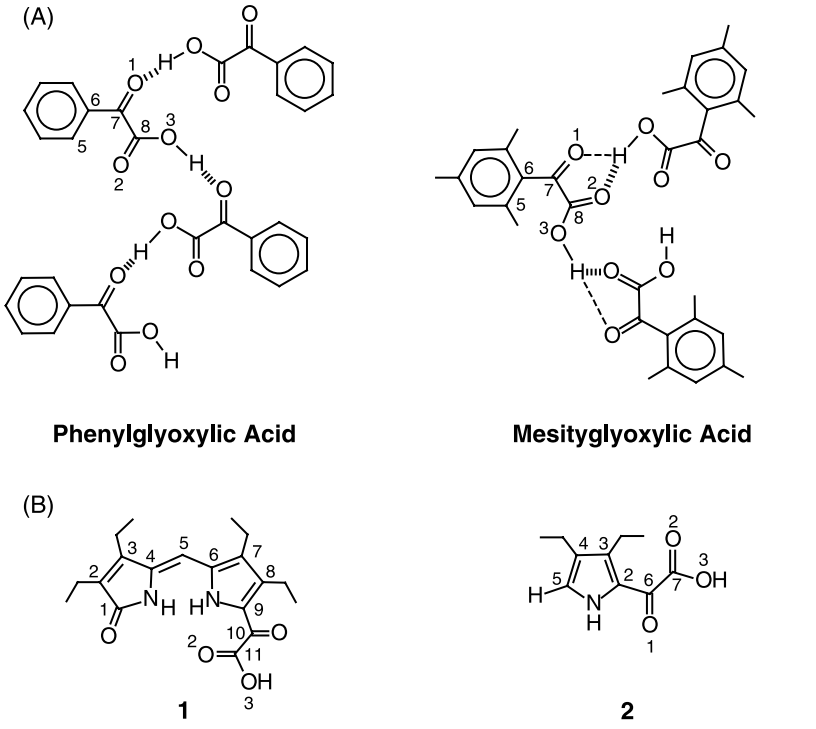

Fig. 1. (A) Intermolecularly hydrogen-bonded catemeric arrays of phenylglyoxylic acid and mesitylglyoxylic acid, as found in their crystals, and partial numbering system used in this work; (B) the target pyrrolylglyoxylic acids of this work and their numbering system

Results and Discussion

Synthesis

Both **1** and **2** were prepared following $SnCl_4$-catalyzed *Friedel-Crafts* acylation of dipyrrinone **3** (to give **1e**) and pyrrole **4** (to give **2e**) with the mono-ethyl ester acid chloride of oxalic acid (Fig. 2). Dipyrrinone **3** [3, 4] and pyrrole **4** [5] were known from earlier work. Saponification of **1e** and **2e** led smoothly to the free acids **1** and **2**.

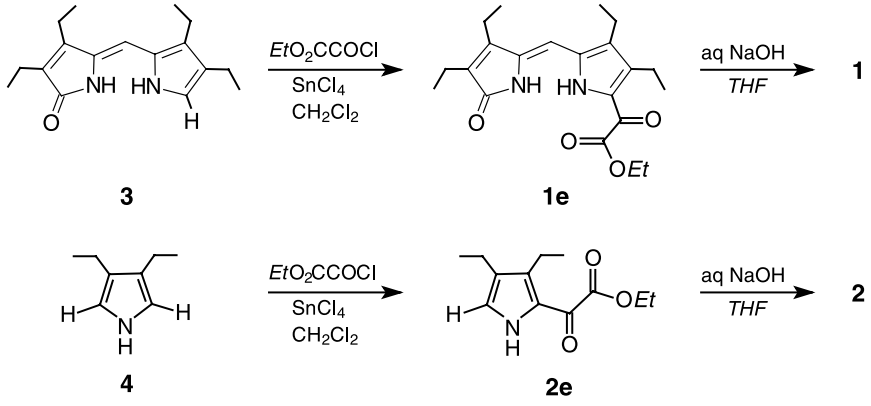

Fig. 2. Syntheses of target compounds **1** and **2** of the work

Table 1. ^{1}H NMR NH chemical shifts in $CDCl_3$ and $(CD_3)_2SO$[a]

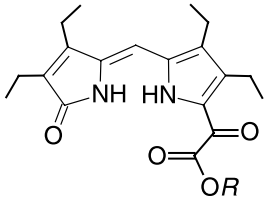

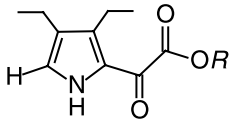

	1 ($R = H$)	**1e** ($R = Et$)	**2** ($R = H$)	**2e** ($R = Et$)
Lactam NH in $CDCl_3$	11.83	10.54	–	–
in $(CD_3)_2SO$	11.14	11.24	–	–
Pyrrole NH in $CDCl_3$	10.01	7.55	10.9	10.33
in $(CD_3)_2SO$	10.52	10.44	11.55	11.66
Acid OH in $CDCl_3$	14.34	–	–	–
in $(CD_3)_2SO$	–	–	14.03	–

[a] Chemical shifts in δ ppm downfield from $(CH_3)_4Si$ at 22°C

Table 2. Molecular weights (*MW*s) of glyoxylic acids **1** and **2** and esters **1e** and **2e** determined by vapor pressure osmometry[a] at 45°C in $CHCl_3$

Compound	Formula Weight (FW) / g mol^{-1}	Measured Weight (MW) / g mol^{-1}
1	344	386 ± 11
1e	386	374 ± 7
2	195	224 ± 10

[a] Calibrated with benzil ($FW = 210$ g mol^{-1}, found $MW = 220 \pm 15$ g mol^{-1}); conc. range: $1.4–5.1 \times 10^{-3}$ mol kg^{-1}

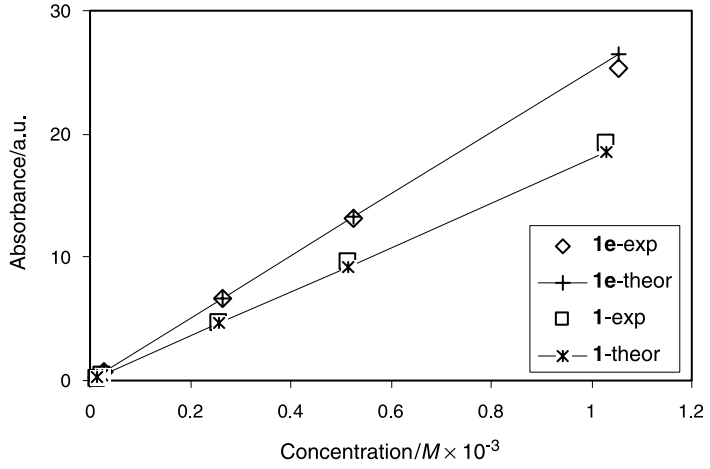

Fig. 3. *Beer*'s law plots of absorbance *vs*. concentration in $CHCl_3$ for dipyrrinoneglyoxylic acid **1** (□, +) and its ethyl ester **1e** (◇, +)

Properties

Acids **1** and **2** and their esters exhibited good solubility in $CHCl_3$. Their structures follow logically from the known precursors (**3** and **4**), and their ^1H and ^{13}C NMR spectra correlate nicely, as expected. The NH chemical shifts (Table 1) are consistent with monomers rather than dimers, and N*O*E studies of **1** and **1e** confirm a *syn-Z*-configuration of the dipyrrinone. Further support of monomeric solutions is found in vapor pressure osmometry (VPO) studies (Table 2) and supported (for **1** and **1e**) by good *Beer*'s Law behavior (Fig. 3).

Configuration in the Crystal

Further support for the constitutional structures of **1** and **2** comes from X-ray crystallography, where **1** is shown to adopt a *syn-Z*-configuration with the ketone and carbonyls *anti* to one another and the ketone carbonyl *anti* to the pyrrole NH (Fig. 4). In this conformation, the α-ketoacid tail of molecule A is linked to the α-ketoacid tail of molecule B in the rare pattern involving two O–H$\cdots$O=C$_\alpha$hydrogen bonds. With the dipyrrinone unit of molecule A also linked

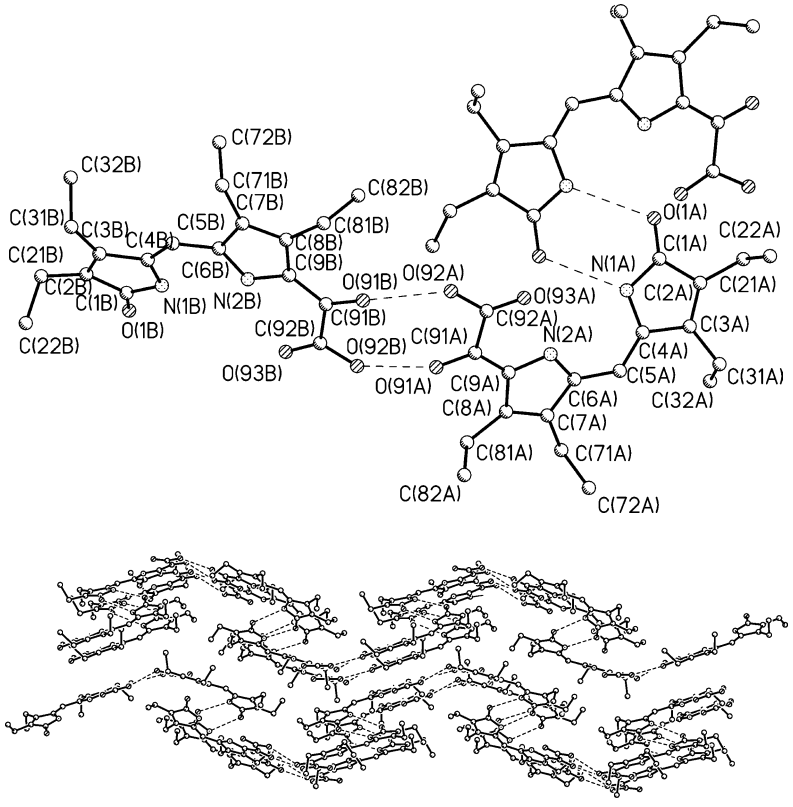

Fig. 4. (Upper) Crystal structure drawing and numbering system of equivalent molecules B and A of **1** showing intermolecular hydrogen bonding between the dipyrrinones of A and B and the unusual intermolecular hydrogen bonding type between the glyoxylic acids of A and B; hydrogen atoms are removed for clarity of presentation; librational ellipsoids have been drawn with 50% probability; (Lower) crystal stacking pattern of **1**

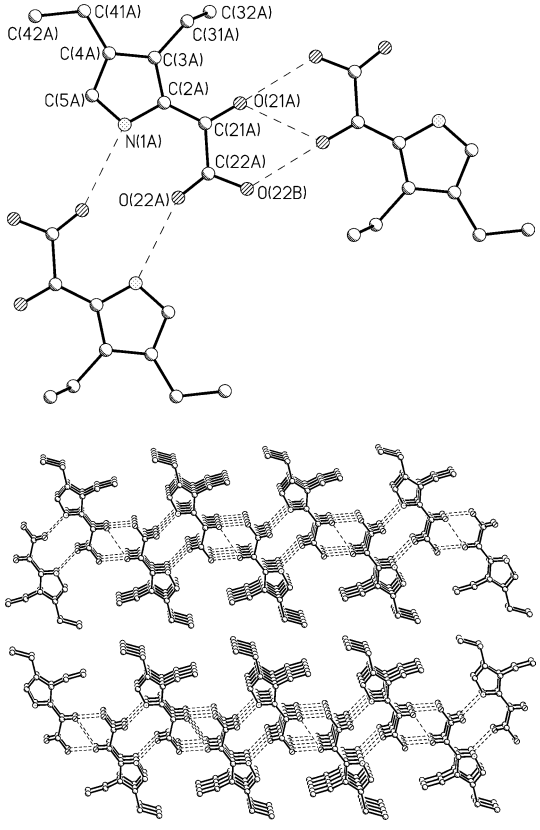

Fig. 5. (Upper) Crystal structure drawing and numbering system of **2** showing the unusual intermolecular hydrogen bonding between the glyoxylic acid groups; librational ellipsoids have been drawn with 50% probability; (Lower) crystal stacking pattern of **2**

to that of molecule B by the typical and characteristic [6] amide-amide hydrogen bonding pattern, **1** forms hydrogen-bonded strands of supramolecular ribbons. The dipyrrinone units of **1** are twisted out of planarity thereby causing the supramolecular ribbons to twist in a stretched helical manner in the crystal.

Pyrroleglyoxylic acid **2** shared the same unique α-ketoacid intermolecular hydrogen bonding pattern as that seen in **1**, along with an intramolecular hydrogen bond between the acid carbonyl and the pyrrole NH. The pyrrole analog **2** is planar, forming supramolecular stacked layers with a $\sim$4.2 Å separation between layers (Fig. 5). The relevant important bond angles and distances for **1** and **2** are shown in Table 3 and compare to those of phenylglyoxylic and mesitylglyoxylic acid (Fig. 1A). One striking difference associated with the intermolecular hydrogen bonding is that the acid OH in **1** and **2** adopts the (less stable) *anti* conformation; whereas, in the phenyl and mesityl analogs it is *syn*. This alone necessitates a different hydrogen bonding arrangement, although in all examples the O–H is hydrogen bonded to the α-keto C=O. Compounds **1** and **2** exhibit the novel pattern of hydrogen bonding shown in Figs. 5 and 6.

Key structure parameters for **1** and **2** may be found in Table 3 and compared with the phenyl- and mesitylglyoxylic acids [1] and with the crystal structure of kryptopyrromethenone which forms a hydrogen bonded dimer in the crystal [7] and

Table 3. Bond distances (d/Å), angles ($\angle$/°), and torsion angles (ϕ/°) from the crystal structures of dipyrrinone-glyoxylic acid **1** (A and B molecules of the unit cell), 2-ethylkryptopyrromethenone (***EKP***), pyrroleglyoxylic acid **2**, and the phenyl- and mesitylglyoxylic acid analogs[a]

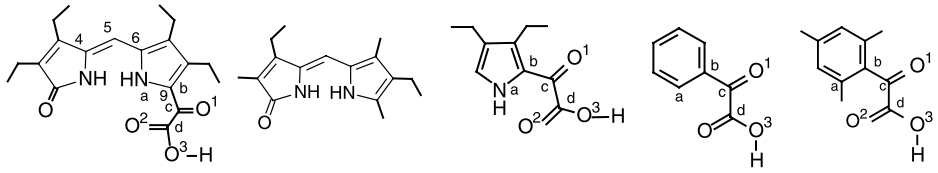

	1		***EKP***[b]	**2**		
	A	B				
ϕ(a-b-c-d)	6.28	0.47		2.1	6.78	129.6
ϕ(O^1-c-d-O^2)	165.6	177.5		170.8	134.3	148.6
ϕ(O^2-d-O^3-H)	161.81	167.1		178.3	0.91	2.58
$\angle$(c-d-O^2)	124.3	124.5		123.7	123.4	121.7
d(c-O^1)	1.235	1.239		1.240	1.217	1.213
d(d-O^2)	1.204	1.205		1.208	1.196	1.221
d(O^1 to HO$^{3'}$)	2.79	2.738		1.97	1.78	2.50
d(O^1 to H-O$^{3'}$)	2.00	1.98		0.93	–	–
d(O^1 to H-O$^{3'}$)	2.22	2.738		2.787	2.686	3.005
d(O^1 to O$^{1'}$)	2.982	2.982		2.907		
ϕ(4-5-6-NP)	4.20	3.60	0.1			
d(LNH to O=CL′)	2.04[c]	2.12[c]	1.97			
d(LN to O=CL′)	2.816[c]	2.850[c]	2.86			
d(PNH to O=CL′)	2.627[c]	2.678[c]	2.09			
d(PN to O=CL′)	3.079[c]	3.279[c]	2.89			

[a] Data from the crystal structures of Ref. [1]; [b] data from the crystal structure of 2-ethylkryptopyrromethenone (***EKP***), a dipyrrinone analog with CH_3 at C(9) (Ref. [7]); [c] distance between lactam (L) or pyrrole (P) of molecule A and molecule B

in solution [6]. No unusual bonding distances or angles are observed, but the ketone C=O bond is slightly longer in **1** and **2** than in the aromatic analogs. The *anti* arrangement of carbonyls within the glyoxylic acid moieties is confirmed; however, the carbonyl groups lie more nearly coplanar in **1** and **2** than in the phenyl and mesityl analogs, where the carbonyls are twisted out of co-planarity by 30–45°. The *ortho*-effect in the mesityl analog causes the glyoxylic appendage to rotate out of planarity with the ring by ~50°; whereas in **1**, **2**, and the phenyl analog it is nearly co-planar. Glyoxylic acid to glyoxylic acid hydrogen bonding distances are similar in **1** and **2**, but slightly shorter in the phenyl analog and considerably (0.2–0.5 Å) longer in the mesityl. The dipyrrinone moiety of **1** is twisted about the C_6–C_5 bond by ~77.8°. In contrast, in the kryptopyrromethenone analog with only a methyl group at C(9) the dipyrrinone is planar, ϕ(4-5-6-N) ~3.9° [7]. The more twisted dipyrrinone of **1** is apparently less able to engage in dipyrrimone to dipyrrinone hydrogen bonding as compared to kryptopyrro-methenone itself. The amide to amide hydrogen bonding distances are similar in both dipyrrinones, but the pyrrole to amide carbonyl distance is ~0.5 Å longer in **1**.

Concluding Comments

A simple pyrroleglyoxylic acid (**2**) exhibits a rare acid to α-keto intermolecular hydrogen bonding pattern, forming hydrogen-bonded supramolecular planar arrays in its crystal. A similar result is found in the dipyrrinone analog **1**, which also engages in amide to amide intermolecular hydrogen bonding to form arrays of supramolecular ribbons in the crystal.

Experimental

NMR spectra were acquired on a Varian Unity Plus spectrometer at 11.75 T magnetic field strength operating at ^{1}H frequency of 500 MHz and ^{13}C frequency of 125 MHz in solutions of $CDCl_3$ (referenced at 7.26 ppm for ^{1}H and 77.23 ppm for ^{13}C) or $(CD_3)_2SO$ (referenced at 2.49 ppm for ^{1}H and 39.50 ppm for ^{13}C). The UV-visible spectra were recorded on a Perkin-Elmer Lambda 12 spectrophotometer. Radial chromatography was carried out on Merck silica gel PF_{254} with $CaSO_4$ binder preparative layer grade, using a Chromatotron (Harrison Research, Inc, Palo Alto, CA) with 1, 2, or 4 mm thick rotors and analytical thin-layer chromatography was carried out on J.T.Baker silica gel IB-F plates (125 μm layer). Melting points were determined on a Mel-Temp capillary apparatus and are corrected. Satisfactory combustion analyses for C, H and N were carried out by Desert Analytics, Tucson, AZ.

The spectral data were obtained in spectral grade solvents (Aldrich or Fisher). The starting compounds 3,4-diethylpyrrole (**4**) [5] and 2,3,7,8-tetraethyl-10*H*-dipyrrin-1-one (**3**) [3, 4] were synthesized according to literature methods.

2,3,7,8-Tetraethyl-10H-dipyrrinone-9-glyoxylic acid ethyl ester (**1e**, $C_{21}H_{28}N_2O_4$)
In a 300 cm^3 round bottom flask equipped with a magnetic stir bar and drying tube CH_2Cl_2 (100 cm^3) was cooled in an ice bath for 30 min. $SnCl_4$ (2.5 cm^3, 21.3 mmol) was added to the solution, and the solution was stirred for an additional 5 min. Oxalyl chloride (2.5 cm^3, 22.3 mmol) was added to the solution, and the solution was cooled for an additional 5 min, at which time a solution of **3** (0.3 g, 1.1 mmol) in 100 cm^3 CH_2Cl_2 was added to the round bottom flask in one portion. The solution was stirred in an ice bath for an additional 30 min, then for 17.5 h at room temperature, protected with a drying tube. The solution was poured into a 1 dm^3 beaker containing 400 g ice and H_2O and the mixture was stirred for 1 h. The organic layer was separated, and the aqueous layer was extracted with CH_2Cl_2 (3×100 cm^3). The combined organic layers were washed with H_2O (4×200 cm^3), dried over Na_2SO_4, and the solvent was removed (rotovap). The residue was purified by radial chromotagraphy (2% CH_3OH–CH_2Cl_2) and crystallized from *n*-hexane-CH_2Cl_2 to give **1e**. Yield 0.28 g (69%); mp 152–153°C; IR (NaCl, thin film): $\bar{\nu} = 3310, 2477, 2933, 2873, 1737, 1702, 1682, 1638, 1213\,cm^{-1}$; ^{1}H NMR ($CDCl_3$, 300 MHz): $\delta = 1.16$ (m, 9H), 1.22 (t, $J = 7.69$ Hz, 3H), 1.43 (t, $J = 6.95$ Hz, 3H), 2.4 (q, $J = 7.69$ Hz, 2H), 2.54 (m, 4H), 2.81 (q, $J = 7.69$ Hz, 2H), 4.39 (q, $J = 6.69$ Hz, 2H), 5.94 (s, 1H), 7.56 (brs, 1H) ppm; ^{13}C NMR ($CDCl_3$, 75 MHz): $\delta = 13.8, 14.2, 14.9, 15.4, 16.4, 17.2, 18, 18.9, 62.9, 95.9, 128.1, 130.1, 132.4, 134.5, 137.8, 140.7, 147.4, 164.2, 168.6, 173.1$ ppm.

2,3,7,8-Tetraethyl-10H-dipyrrinone-9-glyoxylic acid (**1**, $C_{19}H_{24}N_2O_4$)
Dipyrrinone ester **1e** (123 mg, 0.33 mmol) was dissolved in *THF* (100 cm^3). To the solution was added 2 M aq NaOH (30 cm^3), and the solution was refluxed for 40 min, then poured into 150 cm^3 of ice-water. The mixture was stirred and acidified with 10% HCl and extracted with CH_2Cl_2 (3×70 cm^3) and dried over Na_2SO_4. The solvent was removed (rotovap), and the residue was purified by crystallization from *n*-hexane-CH_2Cl_2 to give **1**. Yield 80 mg (70%); mp 154–158°C (dec); IR (NaCl, thin film): $\bar{\nu} = 3165, 3162, 2962, 1682, 1686, 1650, 1272\,cm^{-1}$; ^{1}H NMR ($CDCl_3$, 300 MHz): $\delta = 1.17$ (m, 12H), 2.41 (q, $J = 7.33$ Hz, 2H), 2.59 (m, 4H), 2.82 (q, $J = 7.33$ Hz, 2H), 6.13 (s, 1H), 10.0 (brs, 1H) ppm;

^{13}C NMR (*DMSO*-d_6, 125 MHz): $\delta = 13.5$, 15.3, 15.7, 16.2, 16.3, 16.3, 16.8, 17.3, 94.8, 125.7, 129.4, 131.6, 132.3, 135.7, 135.8, 147.1, 166.7, 172.5, 175 ppm.

3,4-Diethyl-1H-pyrrole-2-glyoxylic acid (**2**, $C_{10}H_{13}NO_3$)

In a 100 cm^3 round bottom flask equipped with a magnetic stir bar and drying tube, CH_2Cl_2 (25 cm^3) was cooled in an ice bath for 30 min. $SnCl_4$ (1 cm^3, 8.5 mmol) was added to the solution, and the solution stirred for an additional 5 min. Oxalyl chloride (1.3 cm^3, 11.7 mmol) was added to the solution and the solution was cooled for an additional 5 min at which time a solution of **4** (1 g, 8 mmol) in CH_2Cl_2 (10 cm^3) was added to the round bottom flask in one portion. The solution was stirred in the ice bath for an additional 30 min then for 18.5 h at room temperature with a drying tube attached. The solution was poured into 200 g ice-water, and the mixture was stirred for 30 min. The organic layer was separated, and the aqueous layer was extracted with CH_2Cl_2 (3×30 cm^3). The combined organic layers were washed with H_2O (4×100 cm^3), dried over Na_2SO_4, and the solvent was removed (rotovap). The residue was purified by radial chromotagraphy (2% CH_3OH–CH_2Cl_2) to give **2e**, which was used directly in the next step. Yield 1.2 g (67%); ^{1}H NMR ($CDCl_3$, 300 MHz): $\delta = 1.14$ (t, $J = 7.69$ Hz, 3H), 1.19 (t, $J = 7.69$ Hz, 3H), 1.41 (t, $J = 6.69$ Hz, 3H), 2.47 (q, $J = 7.69$ Hz, 2H), 2.8 (q, $J = 7.33$ Hz, 2H), 4.37 (q, $J = 7.33$ Hz, 2H), 6.85 (d, $J = 2.93$ Hz, 1H), 10.31 (brs, 1H) ppm.

Ester **2e** (1.2 g, 5.4 mmol) was dissolved in *THF* (75 cm^3). To the solution was added 2 M aq NaOH (35 cm^3), and the solution was held at reflux while stirring for 30 min. Then it was poured into 100 cm^3 ice-water. The mixture was stirred and acidified with 10% HCl, and extracted with CH_2Cl_2 (3×50 cm^3). The organic extracts were combined and washed with H_2O (100 cm^3) and dried over Na_2SO_4. The solvent was removed (rotovap), and the residue was purified by radial chromotagraphy (3% CH_3OH–CH_2Cl_2). The residue was crystallized from CH_2Cl_2 to give 60 mg pure **2**. From the mother liquor, an additional 0.56 g crude product were recovered. Yield 0.62 g (59%); mp 119–121°C; IR (NaCl, thin film): $\bar{\nu} = 3383$, 3243, 2967, 1739, 1623, 1545 cm^{-1}; ^{1}H NMR ($CDCl_3$, 300 MHz): $\delta = 1.15$ (t, $J = 7.33$ Hz, 3H), 1.2 (t, $J = 7.33$ Hz, 3H), 2.5 (q, $J = 7.33$ Hz, 2H), 2.85 (q, $J = 7.33$ Hz, 2H), 7.0 (d, $J = 3.29$ Hz, 1H), 10.9 (brs, 1H) ppm; ^{13}C NMR ($CDCl_3$, 125 MHz): $\delta = 14.3$, 15.1, 17.8, 19.2, 125.4, 128.0, 129.8, 142.7, 163.3, 166.3 ppm.

X-Ray Structure and Solution

Crystals of **1** and **2** were grown by slow diffusion of *n*-hexane into a solution of CH_2Cl_2. A crystal was placed into the tip of a 0.1 mm diameter glass capillary and mounted on a *Bruker* SMART Apex system for data collection at 100(2) K. A preliminary set of cell constants was calculated from reflections harvested from 3 sets of 20 frames for **1** and 3 sets of 150 frames for **2**. These initial sets of frames were oriented such that orthogonal wedges of reciprocal space were surveyed (final orientation matrices determined from global least-squares refinement of 1432 reflections for **2** and 7697 for **1**). The data collection was carried out using MoKα radiation (0.71073 Å graphite monochromator) with a frame time of 20 s for **1** and 120 s for **2** and a detector distance of 4.94 cm. A randomly oriented region of reciprocal space was surveyed to the extent of 2 hemispheres and to a resolution of 0.66 Å. Four major sections of frames were collected with 0.3° steps in ω at 600 different φ settings and a detector position of 36° in 2θ for **1**. The intensity data were corrected for absorption and decay (SADABS) [8]. Final cell constants were calculated from the *xyz* centroids of strong reflections from the actual data collection after integration (SAINT 6.45, 2003) [9]. Crystal data and refinement information for **1** and **2** may be found in Table 4.

The structure was solved and refined using SHELXL-L [10]. The triclinic space group *P-1* for **2** and monoclinic *P2(1)/n* for **1** were determined based on systematic absences and intensity statistics. A direct-methods solution was calculated which provided all non-hydrogen atoms from the E-map. Full-matrix least squares/difference *Fourier* cycles were performed for structure refinement. All non-hydrogen atoms were refined with anisotropic displacement parameters unless stated otherwise. Hydrogen atom positions were placed in ideal positions and refined as riding atoms with relative isotropic displacement parameters (a C–H distance fixed at 0.96 Å and a

Table 4. Crystal data and structure refinement for **1** and **2**

Compound	**1**	**2**
Empirical formula	$C_{19}H_{24}N_2O_4$	$C_{10}H_{13}NO_3$
Formula weight	344.40	195.21
Temperature	100(2) K	100(2) K
Wavelength	0.71073 Å	0.71073 Å
Crystal system	Monoclinic	Triclinic
Space group	*P2(1)/n*	*P-1*
Unit cell dimensions	$a = 8.9250(4)$ Å	$a = 4.1979(8)$ Å
	$b = 17.1317(8)$ Å	$b = 8.3128(16)$ Å
	$c = 24.0284(10)$ Å	$c = 14.538(13)$ Å
	$a = 90°$	$\alpha = 100.668(3)°$
	$\beta = 94.6490(10)°$	$\beta = 95.632(3)°$
	$\gamma = 90°$	$\gamma = 100.551(3)°$
Volume	3661.9(3) Å^3	485.53(16) Å^3
Z	4	2
Density (calculated)	1.249 Mg/m^3	1.335 Mg/m^3
Absorption coefficient	0.088 mm^{-1}	0.099 mm^{-1}
$F(000)$	1472	208
Crystal size	$0.21 \times 0.12 \times 0.06$ mm^3	$0.36 \times 0.04 \times 0.02$ mm^3
Theta range for data collection	1.70 to 32.28°	2.55 to 28.40°
Index ranges	$-13 \le h \le 13$, $-25 \le k \le 25$,	$-5 \le h \le 5$, $-11 \le k \le 10$,
	$-36 \le l \le 36$	$-19 \le l \le 19$
Reflections collected	65074	5055
Independent reflections	13003 [R(int) = 0.1230]	2433 [R(int) = 0.0273]
Completeness to $\theta = 32.28°$ (**1**)	99.8%	
Completeness to $\theta = 28.40°$ (**2**)		99.2%
Absorption correction	SADABS	SADABS
Max. and min. transmission	0.9947 and 0.9818	0.9978 and 0.9645
Refinement method	Full-matrix	Full-matrix
	least-squares of F^2	least-squares of F^2
Data/restraints/parameters	13003/0/459	2433/0/133
Goodness-of-fit on F^2	0.960	1.019
Final R indices [$I > 2\sigma(I)$]	$R1 = 0.0654$, $wR2 = 0.1282$	$R1 = 0.0402$, $wR2 = 0.0927$
R indices (all data)	$R1 = 0.1530$, $wR2 = 0.1623$	$R1 = 0.0717$, $wR2 = 0.1037$
Largest diff. peak and hole	0.492 and −0.421 e.Å^{-3}	0.279 and −0.259 e.Å^{-3}

thermal parameter 1.2 times the host carbon atom). Tables of atomic coordinates, bond lengths and angles, anisotropic displacement parameters, hydrogen coordinates, and isotropic displacement parameters have been deposited at the Cambridge Crystallographic Data Centre, CCDC No. 293010 for **1** and 293011 for **2**.

Acknowledgements

We thank the U.S. National Institutes of Health (HD 17779) for generous support of this research. We also thank the National Science Foundation (CHE-0226402) for providing funding to purchase the X-ray diffractometer used in this work. *NTS* thanks the National Institutes of Health for fellowship support.

References

[1] Chen C-D, Brunskill APJ, Hall SS, Lalancette RA, Thompson HW (2000) Acta Cryst **C56**: 1148
[2] a) Huggins MT, Lightner DA (2000) J Org Chem **65**: 6001; b) Huggins MT, Lightner DA (2001) Tetrahedron **57**: 2279
[3] Bonnett R, Buckley DG, Hamzetesh D (1981) J Chem Soc Perkin **1**: 322
[4] Huggins MT, Lightner DA (2000) Tetrahedron **56**: 1797
[5] Sessler JL, Mozaffari A, Johnson MR (1998) Organic Syntheses Coll Vol IX: 242
[6] Huggins MT, Lightner DA (2001) Monatsh Chem **132**: 203
[7] Cullen DL, Black PS, Meyer EF, Lightner DA, Quistad GB, Pak C-S (1977) Tetrahedron **33**: 477
[8] Sheldrick GM (2003) SADABS, V6.14, Bruker Analytical X-rays Systems, Madison, WI, USA
[9] SAINT V6.45, Bruker Analytical X-ray Systems, Madison, WI, USA
[10] Sheldrick GM (2003) SHELXT-L V6.14, Bruker Analytical X-ray Systems, Madison, WI, USA